

# Contents

<b>1</b>	<b>Boson sampling: development of hybrid beam splitter</b>	<b>2</b>
1.1	Theoretical background [1] . . . . .	2
1.2	The first simulation attempt . . . . .	3
1.3	Importance of property grounding . . . . .	6
1.4	Curvature radius . . . . .	10
1.5	Totally . . . . .	12
<b>2</b>	<b>First fabrication of BS</b>	<b>14</b>
2.1	Fabrication 23.02.18 . . . . .	16
2.2	SPR dose test . . . . .	17
2.3	Etching test for aluminum dry system . . . . .	20
2.4	Al dry etching . . . . .	20
<b>3</b>	<b>AZ-resist test</b>	<b>20</b>
3.1	Airbridges fabrication . . . . .	23
3.2	Beam splitter#2 . . . . .	27
<b>4</b>	<b>Measurement of a beamsplitter</b>	<b>30</b>
4.1	Measurement result . . . . .	31

# 1 Boson sampling: development of hybrid beam splitter

## 1.1 Theoretical background [1]

For boson sampling properties an element which can entangle pairs of photons is required. For this propose a hybrid beam splitter is typically used. The beam splitter has 2 inputs and 2 outputs with phase difference in 90 degree. It consists of 4 branches, 2 of them has input impedance, i.e. 50 Ohms, another 2 has input impedance/4. The length of each branch is determined by the working frequency of the beam splitter: the length =  $\lambda/4$ , where  $\lambda$  is working wave length.

The output characteristics are following: transmission coefficient  $S_{12}$  and  $S_{13}$  are 0.5, or -3dBm in logarithmic scale. For other 2 ports the reflection  $S_{11}$  and transmission  $S_{14}$  is close to 0, or  $\rightarrow \infty$  in logarithmic scale. The characteristics are shown in fig. 1

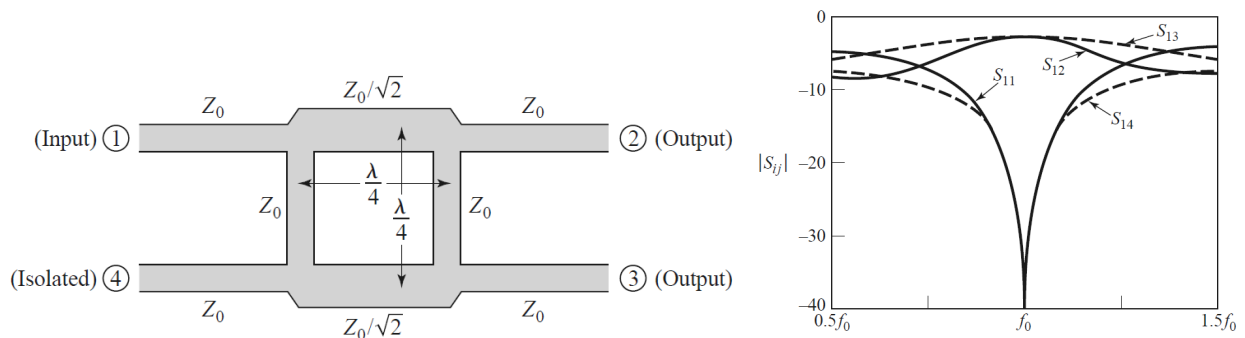


Figure 1: On the left picture the principle scheme of hybrid microwave beam splitter is shown: two branches with the same impedance as the input line (50 Ohms) and two lines with impedance  $50/\sqrt{2}$  are shown. On the right side outputs characteristics are shown.

Also output characteristics can be expressed by transmission and reflection wave with odd and even modes (fig. 2)

$$\begin{aligned}
B_1 &= \frac{1}{2}\Gamma_e + \frac{1}{2}\Gamma_o, & B_1 &= 0 && (\text{port 1 is matched}), \\
B_2 &= \frac{1}{2}T_e + \frac{1}{2}T_o, & B_2 &= -\frac{j}{\sqrt{2}} && (\text{half-power, } -90^\circ \text{ phase shift from port 1 to 2}), \\
B_3 &= \frac{1}{2}T_e - \frac{1}{2}T_o, & B_3 &= -\frac{1}{\sqrt{2}} && (\text{half-power, } -180^\circ \text{ phase shift from port 1 to 3}), \\
B_4 &= \frac{1}{2}\Gamma_e - \frac{1}{2}\Gamma_o, & B_4 &= 0 && (\text{no power to port 4}).
\end{aligned}$$

Figure 2: On the left picture output characteristics are expressed by odd and even modes of a wave. On the right picture output characteristics in complex coordinates are shown.

The total scattering matrix is presented in fig. 3

$$[S] = \frac{-1}{\sqrt{2}} \begin{bmatrix} 0 & j & 1 & 0 \\ j & 0 & 0 & 1 \\ 1 & 0 & 0 & j \\ 0 & 1 & j & 0 \end{bmatrix}$$

Figure 3: The total scattering matrix of a hybrid beam splitter.

## 1.2 The first simulation attempt

The investigation was started from drawing a design and simulation it in some microwave software like a Microwave office placed in Tokyo University of Science. Drawing design is performing by usage macros functions of Layout Editor[2]. The first version of beam splitter and its performance is depicted in fig. 4. This design was performed without air bridges.

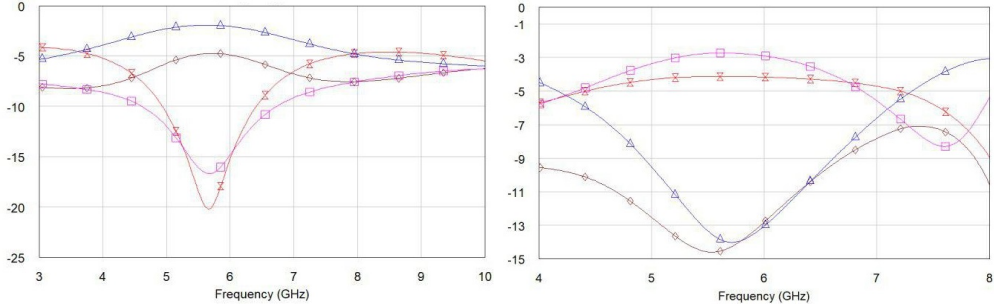


Figure 4: Performance of a beam splitter without common grounding (air bridges). [On edges the ground is negative "-1"]. There is no guarantees that polygons have the same potential.

In this picture it is clearly seems transmission to different ports [S12 and S13] is significant different. Also, the reflection peak is wide and is not so deep. After that common grounding was added. The result after adding air bridge is depicted in fig. 5.

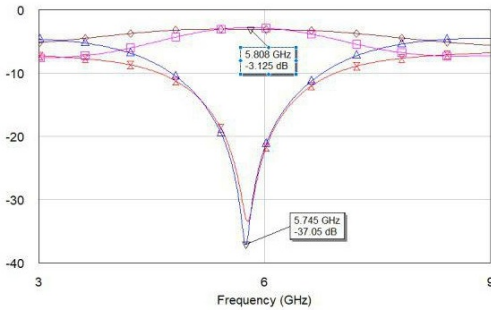


Figure 5: Performance of the same splitter but with common grounding (using air bridges).

In this picture it is clear that the working frequency is shifted off expectation frequency (5.745 GHz vs 6 GHz, the shift is 255 MHz). For transmission signal the result (-3.125 dBm) is quiet close to the ideal case of -3.0dBm.

Reasons of this shift can be following:

1. Influence of air bridges
2. Influence of the T-junction shape (see fig. 6)
3. Influence of changing effective length due to meanders shape of each branches.

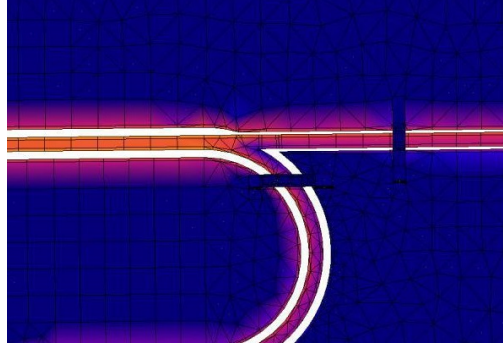


Figure 6: An example of T-junction [already with air bridges]. Colours shows current density distribution [Microwave Office.]

Let's discuss about these possible reasons. **The influence of air bridges** (additional cross talk between air bridges and coplanar wave guides of each branch) is negligible for simulations (but may be not for experiment) because there is the same shift before and after air bridge additional.

Change of the effective length **due to meander curvature** is possible to calculate using the following formula [3]:  $R_{eff} = R_{inner} + 0.3 * W = R_{math} - 0.2 * W$ , if  $3 < R/W < 7$ , where R and W are curvature radius and width of a coplanar wave guide (only width, without gap; in our case is 2 and 4). Each meander step accumulate an effective decreasing length of  $0.2 * W$ . Typical amount of meander steps are 5-21 for splitting line ( $W = 3\text{um}-27\text{um}$ ) and are 15-71 for feeding line ( $W = 1\text{um}-9.5\text{um}$ ). Totally, it should be expected an additional length of  $(13 * 15\text{um} + 43 * 5\text{um}) = (195\text{um} + 215\text{um})/2 = 205\text{um}$  and it is equal to  $f_{new} = \frac{205*(6*10^9)^2*4*\sqrt{12.8/2}}{3*10^8} = 248.35 \text{ MHz}$ , which is close enough to 255MHz of shifting. However, the shift should decrease the length of branches and working frequency should be increased. But there is the opposite situation. To sum up, there is a possible reason to shift working frequency, but there are other reasons, at least one.

Another possible reason of the shift is a **shape of T-junctions**. As seems in fig. 7 on a current distribution map there are some "reflections" and "penetrations" of current density. It can cause leakage of electrical field in T-shape junctions. Unfortunately, to make a numerical estimation of the influence is not possible.

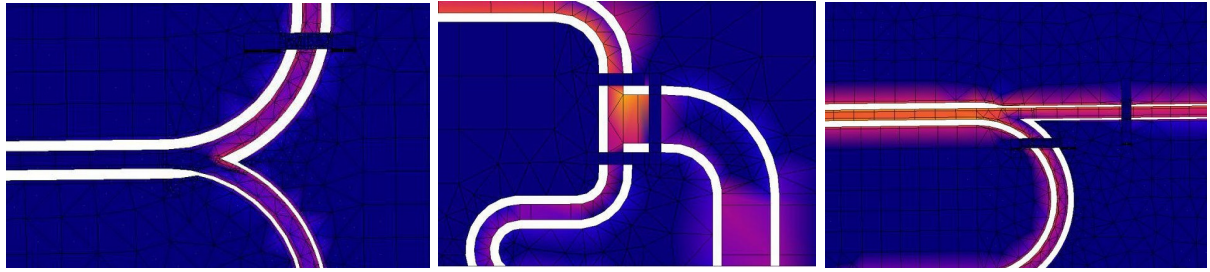


Figure 7: Variability of different T-junction shapes on a map of current distributions.

Importance of the proper grounding will be discussed in the next subsection.

### 1.3 Importance of property grounding

It is possible to make the equal potential between central and other parts using air bridges (see fig. 8)

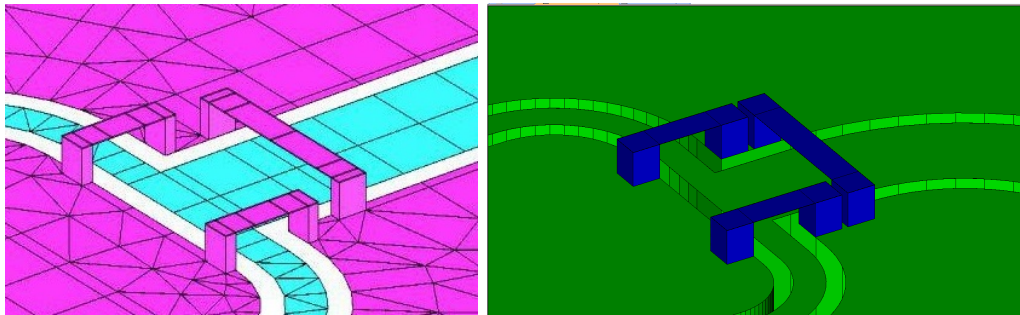


Figure 8: Simulation example of air bridge concept. Bridges are placed near a T-junction.

There are various of simulation tests. First ones are dedicated by investigation of usage airbridges. [Technical details: Sample named "curve..clear..006" was used [using "via" function – it means thickness is  $0.05\mu m + 450\mu m$  – is significant different]. Parameters:  $h=1.006$ ,  $wfeed = 42e3$ ,  $gfeed = 25e3$ ,  $wsplitter = 140e3$ ,  $gsplitter = 25e3$ ,  $meanderSegmentsplitter = 133e3$ ,  $meanderSegmentfeed = 150e3$ ]

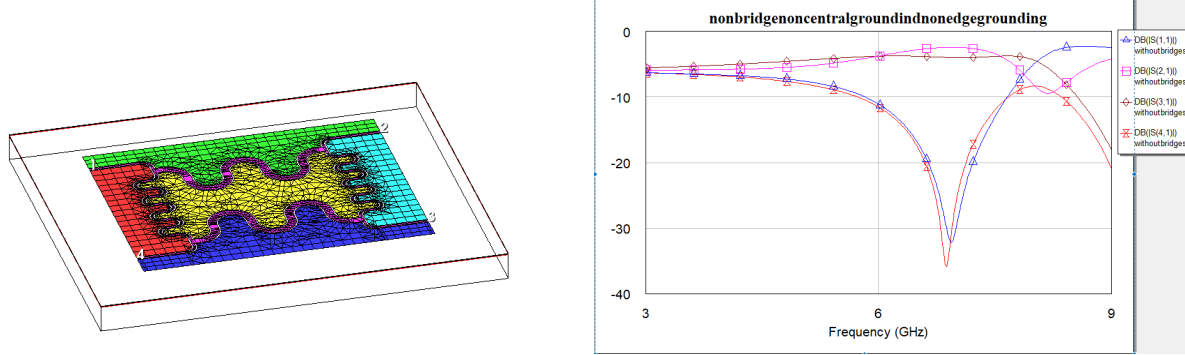


Figure 9: Simulation BS without any grounding and airbridges. The working frequency is significant shifted. Also there are some noises before working frequency band. The geometry was changed in comparison with fig.5.

Without any grounding and air bridges the working frequency is significantly shifted and there is unpredictable noise during working frequency band (see fig. 9).

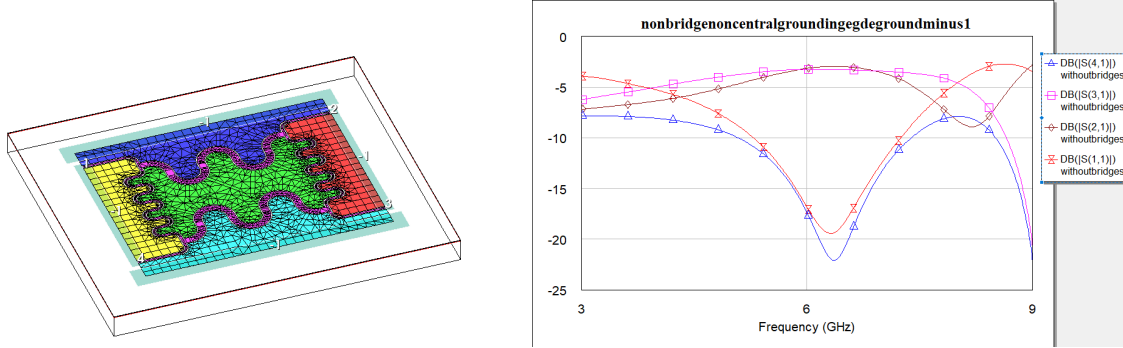


Figure 10: Simulation BS without air bridges and without "via" function in central part. Edge grounding is negative, named "-1".

Added edge grounding using negative port "-1" (see fig. 10). It looks like several negative port "-1" cause grounding with not the same potential: peaks are shifted and blurred.

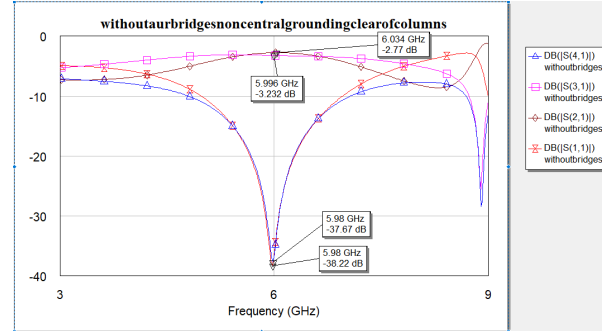
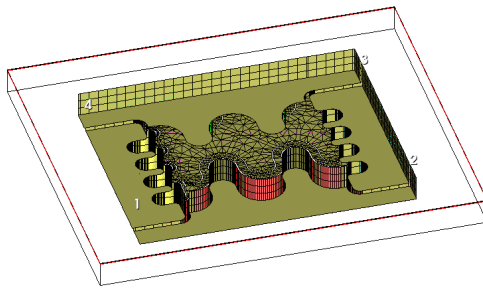


Figure 11: Simulation BS without air bridges without "via" in central part. Edge grounding is the same due to "via".

Fig. 11 shows performance of a BS using edge grounding "via" function without airbridges. In comparison with the previous results this graph looks better, but noise is here.

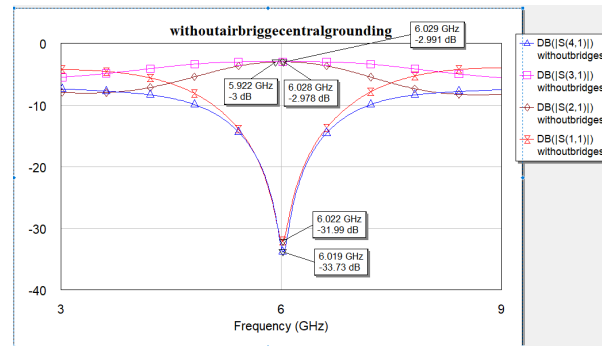
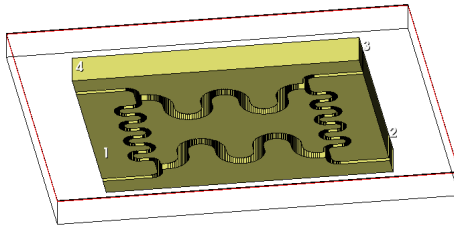


Figure 12: Simulation BS without airbridges with artificial central part grounding (using "via").

Usage "via" function allows to get quiet well symmetrical response without noise (see fig.12). This functionality play role of the "artificial grounding" during a substrate to PCB board. It means that metal thickness is equal to sum of metal thickness (0.05um) and substrate thickness (450um).

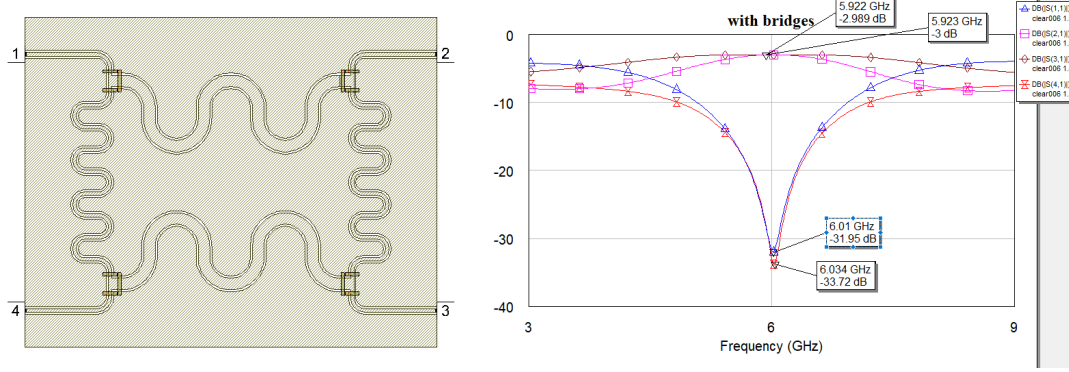


Figure 13: Simulation of BS with air bridges without "via" in central part.

This is results of the usage airbridges for grounding central part without "via" function (see fig. 13, edge grounded by "via").

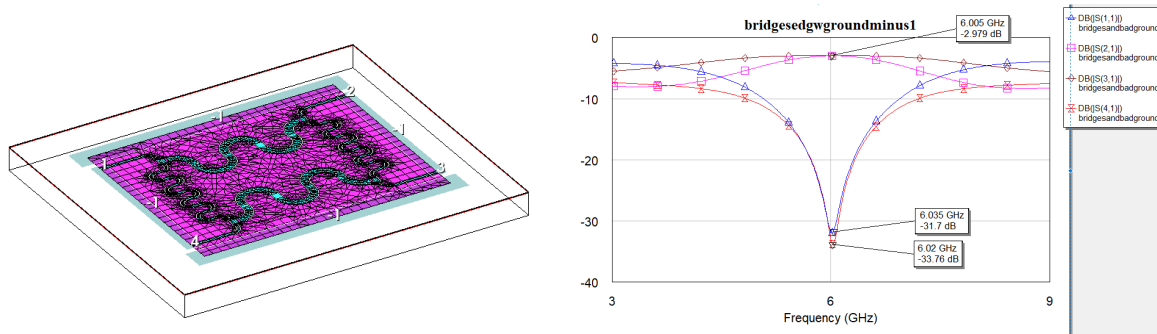


Figure 14: Simulation BS with air bridges without "via" in central part and grounding edge part using negative ports "-1".

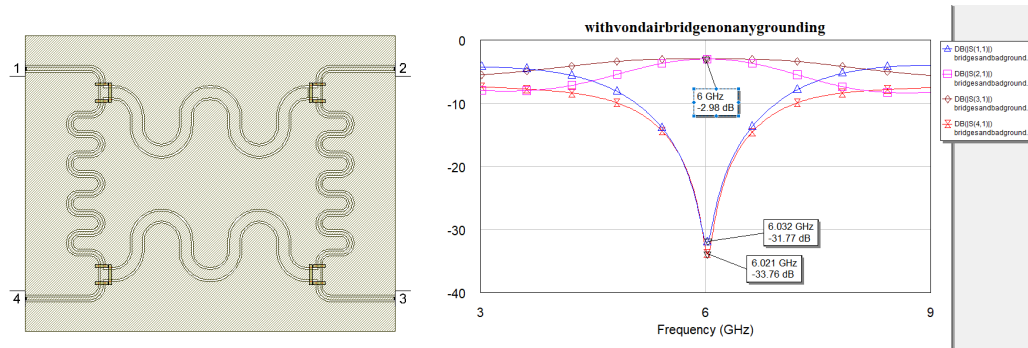


Figure 15: Simulation BS with air bridges without "via" in central part and without any ground.

Finally, in the fig. 14 results with bridges with negative edge grounding are shown and in fig. 15 results with airbridges without any grounding are shown. It seems like what we actually expect to see. It means that it is not so important type of edge grounding if the airbridges exist and work. This results shows powerful of airbridges. On real experiments we can't say properly about edge grounding. In the simulation case it is ideal model without any losses with ideal potential distribution. In real life it can be not absolutely true. To avoid any dependencies on edge grounding environment it is naturally to use airbridge to get a robust system. Summary results are shown in the table. 1.3.

ground properties	No bridges, GHz (dBm)	Yes bridges, GHz (dBm)	No bridges, but "via", GHz (dBm)
No any ground	-	6.032(-31.77), 6.021(-33.76), -2.98	-
Ground edge by "-1" ports	-	6.035(-31.7), 6.02(-33.76), -2.979	-
Ground edge by "via"	5.98 (-37.67), 5.98 (-38.22), -2.77/-3.232	6.01(-31.95), 6.034(-33.72), -3/-2.989	6.22(-31.99), 6.019(-33.73), -2.991/-2.978

Table 1: Total parameters sets of simulations airbridge influence.

Another interesting point where is the most optimal place to put airbridges. For example, it will be interesting to measure BS with different displacement of the bridges:

1. only near T-junctions
2. only in the lines center
3. with both bridges
4. without any bridges.

THE SECTION IS DEVELOPING

## 1.4 Curvature radius

Using more sharp curvature radius can decrease total size of a design, but there is possibility of electrical field leakage. There is measured characteristic of 2 the same beamsplitter, except curvature radius (2w and 4w) (see fig. 16 and fig. 17)  
 FIND DATA: THE SECTION IS DEVELOPING

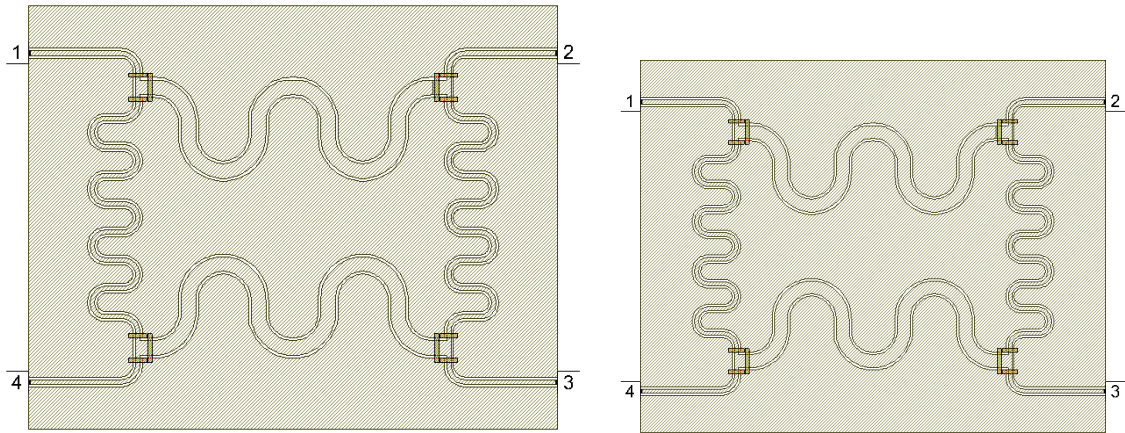


Figure 16: Measurement characteristics of a BS with radius curvature is  $2w$ .

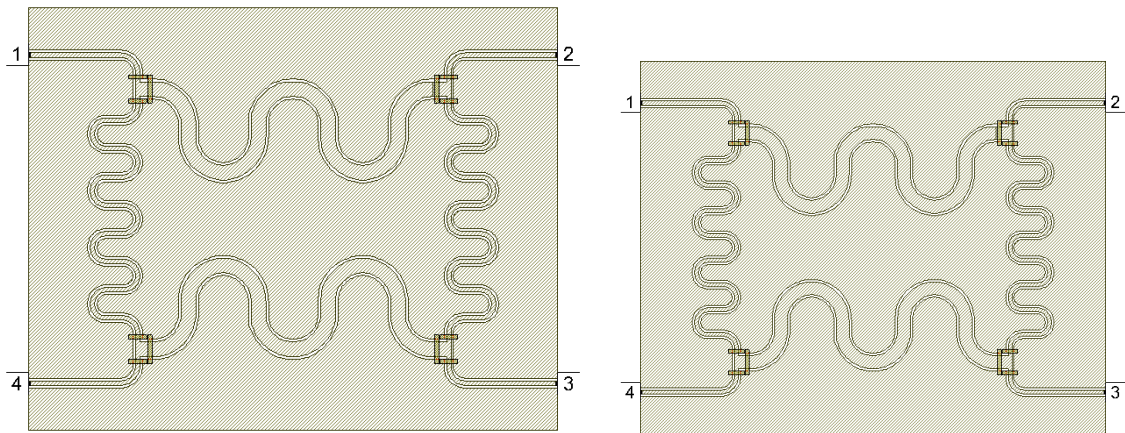


Figure 17: Measurement characteristics of a BS with radius curvature is  $4w$ .

Also it is interesting a compare of fig 18.

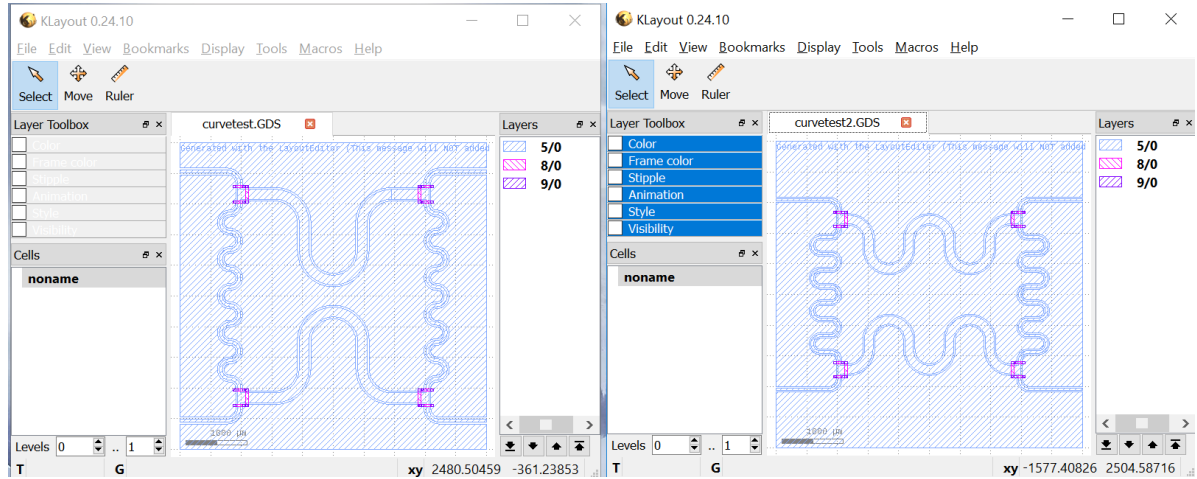


Figure 18: Measurement characteristics of a BS with different meander length.

## 1.5 Totally

To sum up, there are several important points, which should be taken into account before design of a beamsplitter:

1. Make proper ground using air bridges.

In this case the effective length and working frequency can little change.

Otherwise: crucial frequency shift and blurring of working frequency.

2. Different T-junction shape

Otherwise: leakage of the electrical field, more losses in transmission and reflection signal

3. Absolute size of the coplanar wave guide and gap

Otherwise: penetration of the electrical field, possibility of changes working frequency and increasing of losses

4. Using meanders to make BS more compact

Otherwise: more losses and shift of working frequency

The best beamsplitter characteristics is shown on fig. 19.

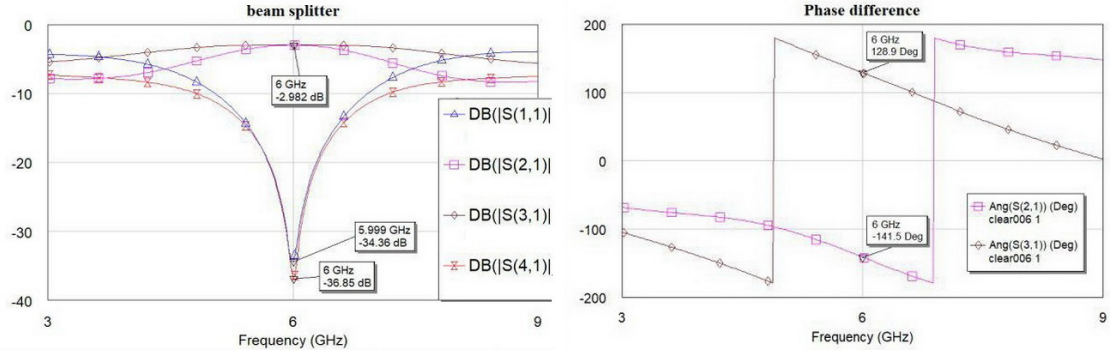


Figure 19: Final simulation characteristics. On the right graph is amplitude measurements.  $S_{21}=S_{31} = -2.982\text{dBm}$ ,  $S_{11} = -34.36\text{dBm}$ ,  $S_{41} = -36.85 \text{ dBm}$ . On the right figure is shown phase measurement. There is a phase shift is  $89.6^\circ$ ( $-270.4^\circ$ ). The used software is Microwave Office.

## 2 First fabrication of BS

For the ideal case it will be better to use huge design for beam splitter – for this case the accuracy of width line (and impedance mismatching) is better, also small airbridges is difficult to fabricate. Or another hand the size of a substrate is quiet small 2.5mm x 5 mm. Furthermore, majority space of a substrate will be occupied by single-photon sources. To totally we can use just approximately 2mm x 2mm. This is the reason why it is important for us to use small beamsplitter. Please see fig. 20.

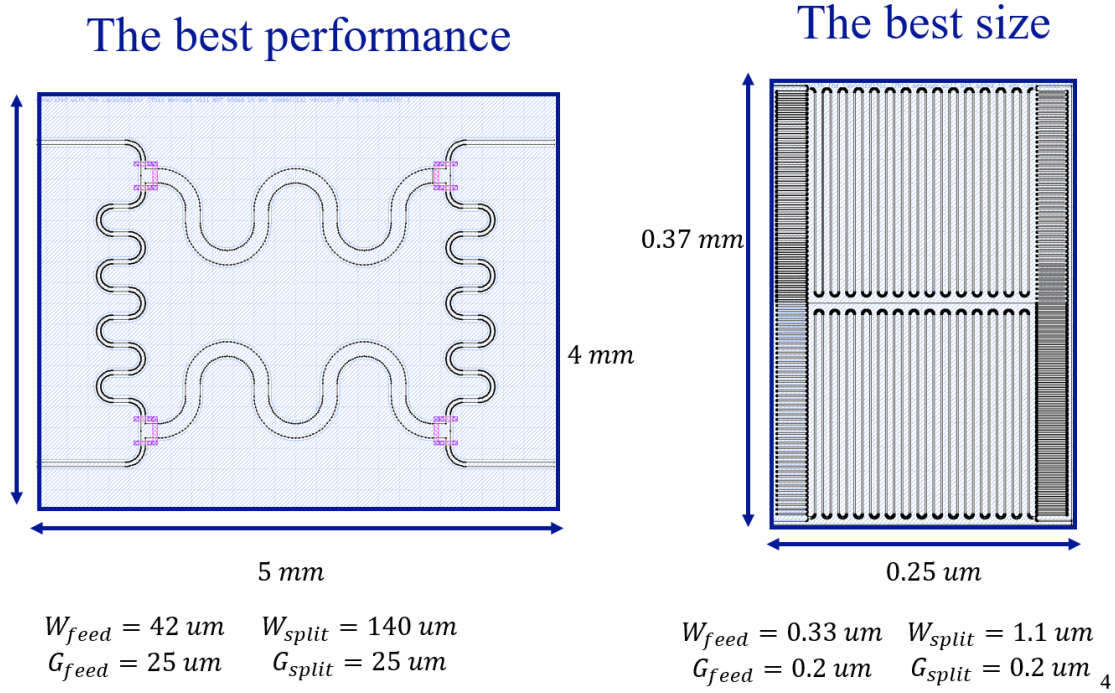


Figure 20: The reason to use and not to use small beam splitters.

To check simulation parameters and to understand what is the most crucial parameters the test will be conducted. For this test the follow parameters will be checked:

1. Absolute size of gaps and waveguide width (from "Micro" to "Meter")
2. Curvature radius (from  $2w$  to  $4w$ , where  $w$  is waveguide width)
3. Different effective length (with hint coefficient from 1 to 1.006)

The total set parameters is shown in a table 2.

Parameters [um]	"Micro"	"Centi"	"Center"	"Meter"
feedline width	1	1.9	4.25	9.5
gap width	0.55	1	2.5	5
splitline width	3	5.5	11	27
splitgap width	0.55	1	2.5	5
split meanders length, radius curvature=4w of lines, h=1.006	272	342	275	275
feed meanders length, radius curvature=4w of lines, h=1.006	51.09	68.05	137.3	155.5
split meanders length, radius curvature=2w of lines, h=1.006	157.5	213	342	435
feed meanders length, radius curvature=2w of lines, h=1.006	46.49	63.15	72.1	104
split meanders length, radius curvature=2w of lines, h=1	156	210	340	432
feed meanders length, radius curvature=2w of lines, h=1	46.17	62.7	71.52	103
split meanders length, radius curvature=4w of lines, h=1	270	338	270	270
feed meanders length, radius curvature=4w of lines, h=1	50.7	67.5	136.15	232

Table 2: Total parameter sets of testing different BS designs

The set of design is here (see fig. 21):



Figure 21: Full set of design: on the left side is set with colours for navigation, on the right side the total design on a 2-inch wafer is placed.

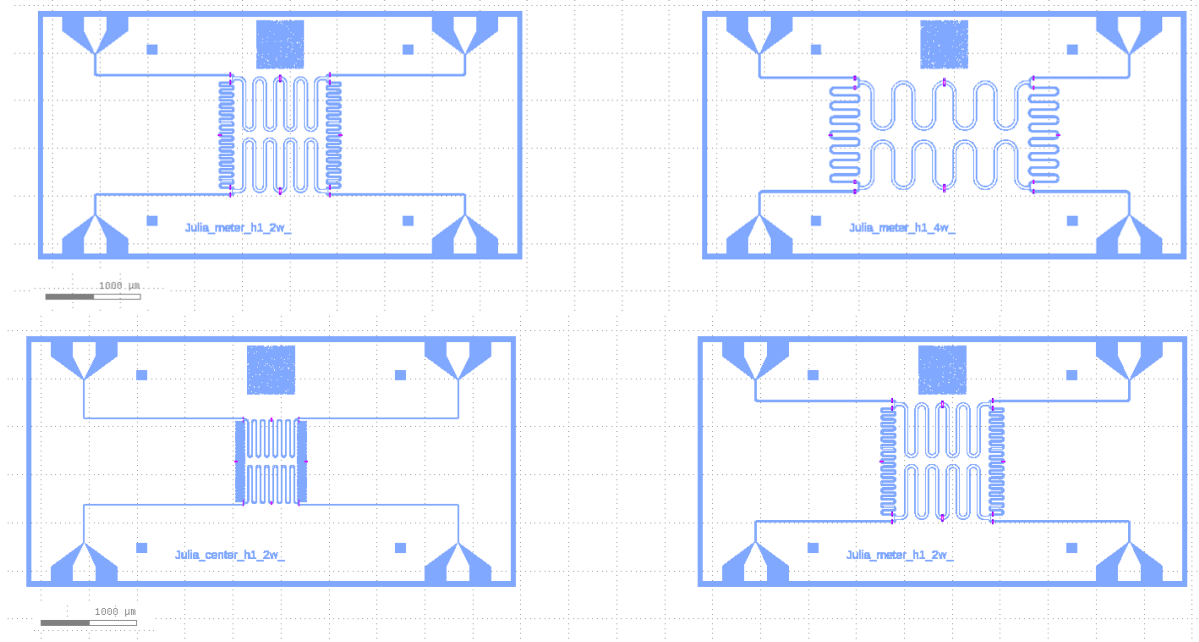


Figure 22: Different changeable parameters: the curvature radius (two top pictures), absolute size of wave guide (two bottom pictures) and with additional coefficient (is not presented here).

All of this samples will be fabricate on the undoped silicon wafer with 2-inch size. All samples will be fabricated with air bridges, which sizes is correlated by the width of the coplanar waveguides:  $\text{air length} = 1.4 * \text{width of feedline} + 2\text{pad's length} + 1\mu\text{m}$ .

## 2.1 Fabrication 23.02.18

The best performance will be using electron-beam lithography. It is crucial important to substrate for real experiment, but for developing technology it is quiet long and too complicated. Due to these reasons I used optic maskless system DL1000SG/RWS placed in RIKEN. For the first attempt of the optic lithography with general property parameters (SPR220-3.0, lithography dose  $170\text{mJ/cm}^2$ , developing 3 min in AZ developer) gets extremely extended lines, some of lines even sticks together, see fig. 23.

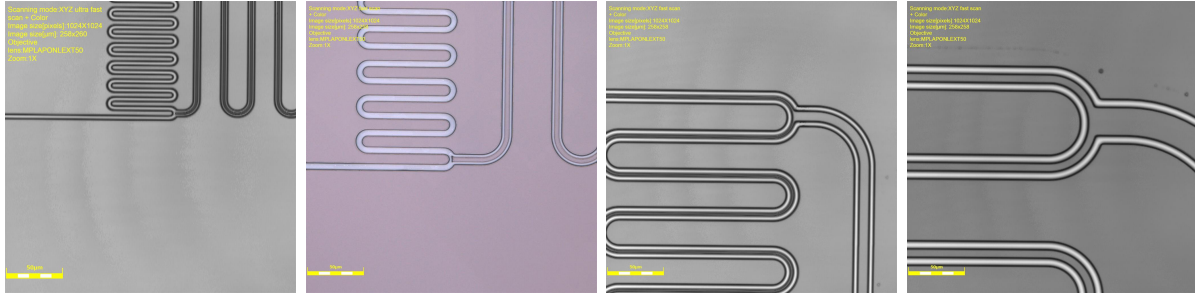


Figure 23: Fabrication with usage SPR220-3.0 resist with expose dose of  $170mJ/cm^2$ , developing time is 3min. From left to right: "micro", "centi", "center", "meter".

From these pictures it is clear that huge overexposure or overdeveloping is here. There are two possible ways: the first one is just changing design size or try to find the most accuracy parameters. For second case we can make a dose test.

## 2.2 SPR dose test

We can make a dose test with this design see fig. 24.

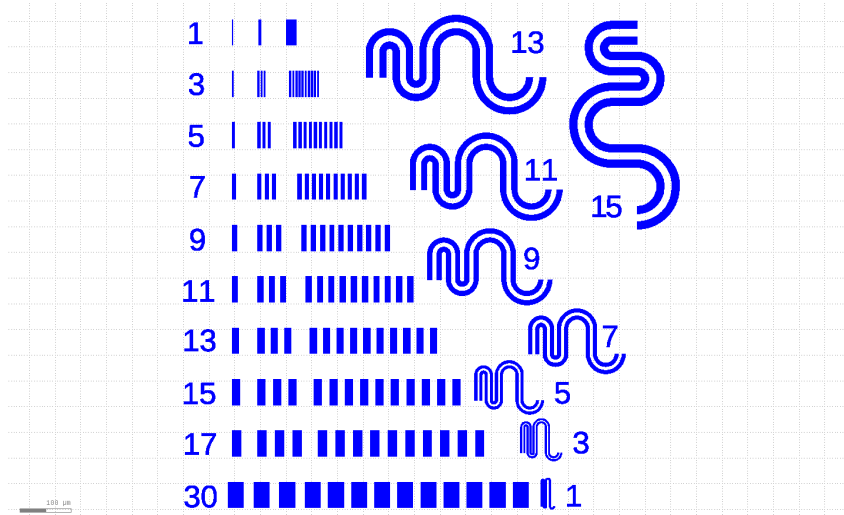


Figure 24: Design for optic dose test. The numbers mean the width of each line in microns. The distance between lines is the same with width of lines. Totally size is 1mm x 1mm.

For dose test was conducted several tests. First one with dose range from  $170mJ/cm^2$  to  $100mJ/cm^2$ , the dose step is  $10mJ/cm^2$ . The result is following: width lines with all regimes is the same. It means it is required extended range. The new regime is from

$450mJ/cm^2$  to  $50mJ/cm^2$  with the step of  $50mJ/cm^2$ . The most accuracy result with dose  $50mJ/cm^2$ , but for width of 1um here is under developing. It can be due to the height of the resist is 3um. It is very high and thin column.

The next step is to try another developing regime with the same expose dose ( $300mJ/cm^2$ - $30mJ/cm^2$ ). Developing time would be from 1min to 3 min.

The result is follow: the best developing time is 3 min. The best resolution with approximately the same design is 3um (see fig.25).

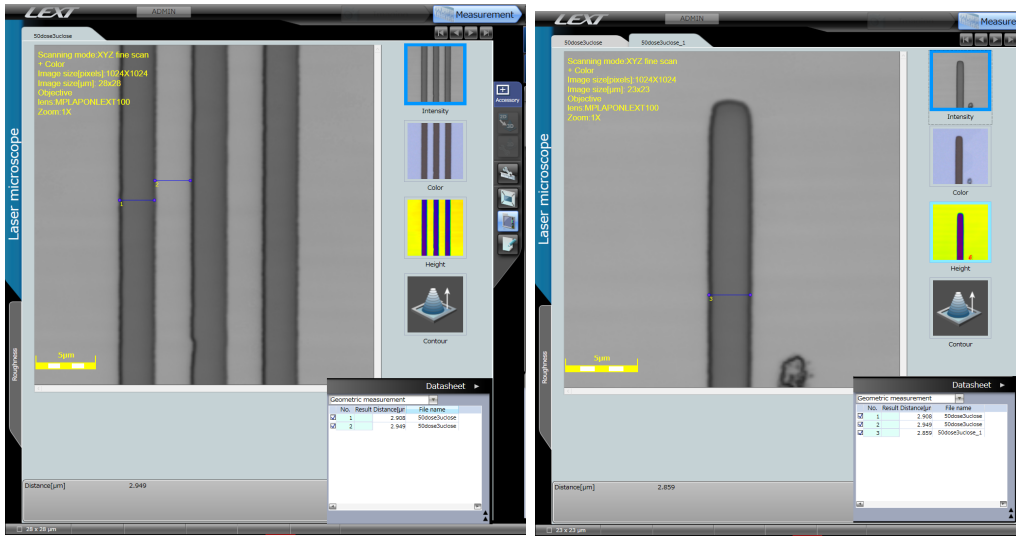


Figure 25: Optic photograph of the fabricated strips: left picture with proximity effect, right one is a single strip. The measured width are 2.91um and 2.86um with design of 3um [Optic photo is made by using "Olympus lext" software].

Here is comparison of two different dose:  $170mJ/cm^2$  and  $50mJ/cm^2$  (see fig.27).

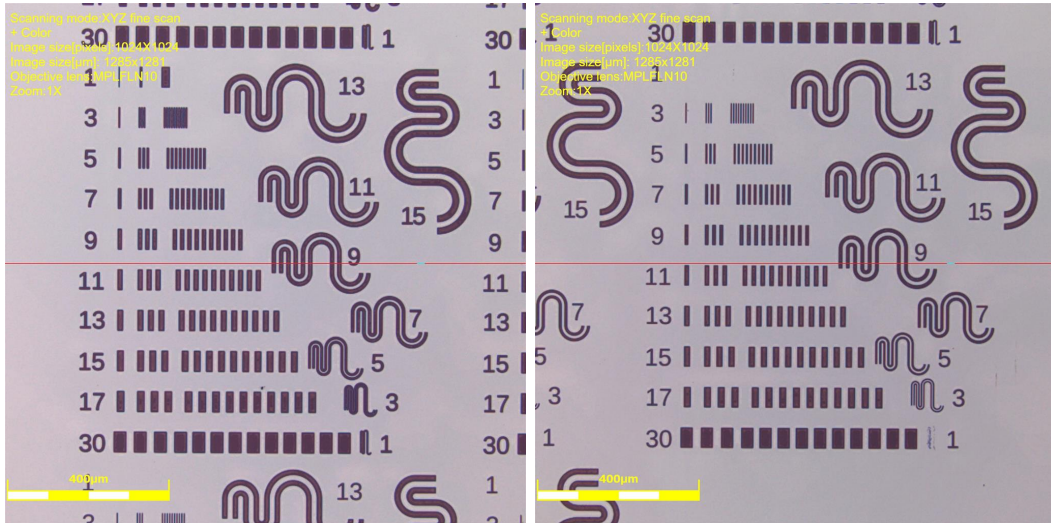


Figure 26: Comparison between different doses:  $170\text{mJ}/\text{cm}^2$  and  $50\text{mJ}/\text{cm}^2$ . The difference is the most obvious on 9um and 11um lines.

This result is not absolutely ideal. **The best choice is to use  $60\text{mJ}/\text{cm}^2$ .**

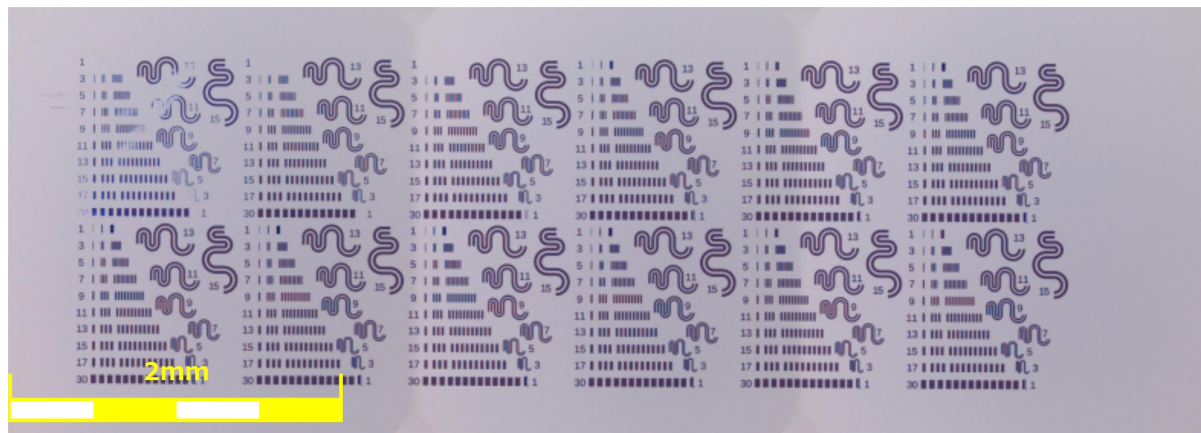


Figure 27: Full photo of the different dose AZ resist with the same design.

**IMPORTANT:** for any dose you must take into account a design for a exposure dose. Resist thickness, geometry of a pattern and total square can crucial influence to the best exposure dose number. The manifestation of this phenomena you can see in fig. 28, so called proximity effect.



Figure 28: Manifestation of the proximity effect. The exposed area is different due to some interference into resist.

The next step is usage this dose to fabricate coplanar part of beam splitters.

### 2.3 Etching test for aluminum dry system

For this test the same dose test design was used with lithography dose of  $60mJ/cm^2$ , but after developing lines looks [from optic microscopy] like extended. May be it is due to aluminum is better reflect light and interference blemish the real size of the lines. Let's see after dry etching.

### 2.4 Al dry etching

Full bulk of aluminum was etched in 3min 45sec (4min to be sure that etching is almost done) in the solvent 30deg with "medium" [ $\approx 1$  round per second] rotation. Exactly the same way was used to the real device (beamsplitter#1 1-10 Ohms).

## 3 AZ-resist test

Due to SPR resist is very thick it was decided to try another resist: AZ1500. Minimal thickness of SPR 3.0 is 2.5-3um (5000RPM). Minimal thickness of AZ1500 is 1.2um (5000RPM). SPR resolution 2.5um. AZ resolution 1um. The parameters of working with AZ resist are: 5000rpm(2slope+5s rpm500 3slope 50s rpm5000 5slope), HP 115deg 3min, the lithography dose is  $80mJ/cm^2$  developing AZ developer:Water = 1:1 90sec. The best pics fig. 40.

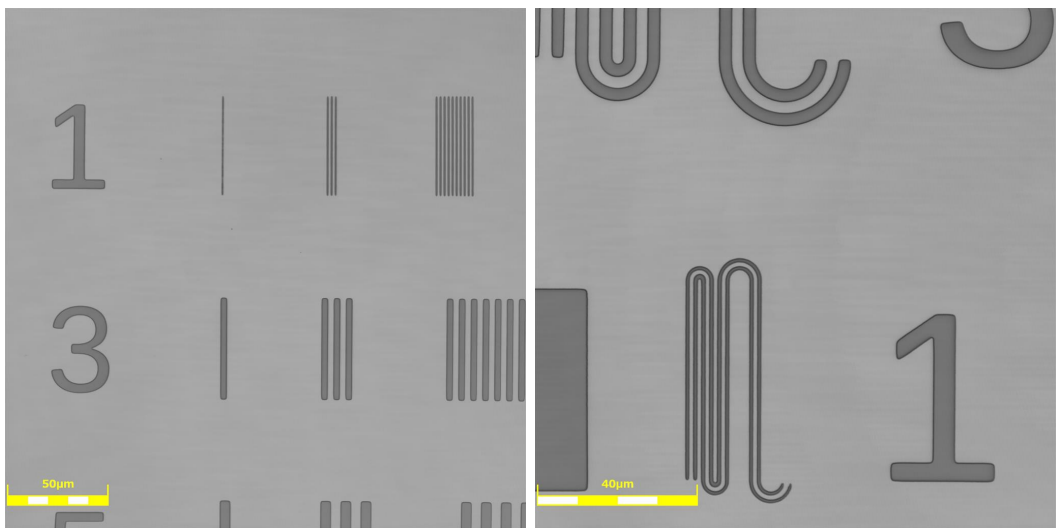


Figure 29: AZ resist test. The resist thickness is 1um.

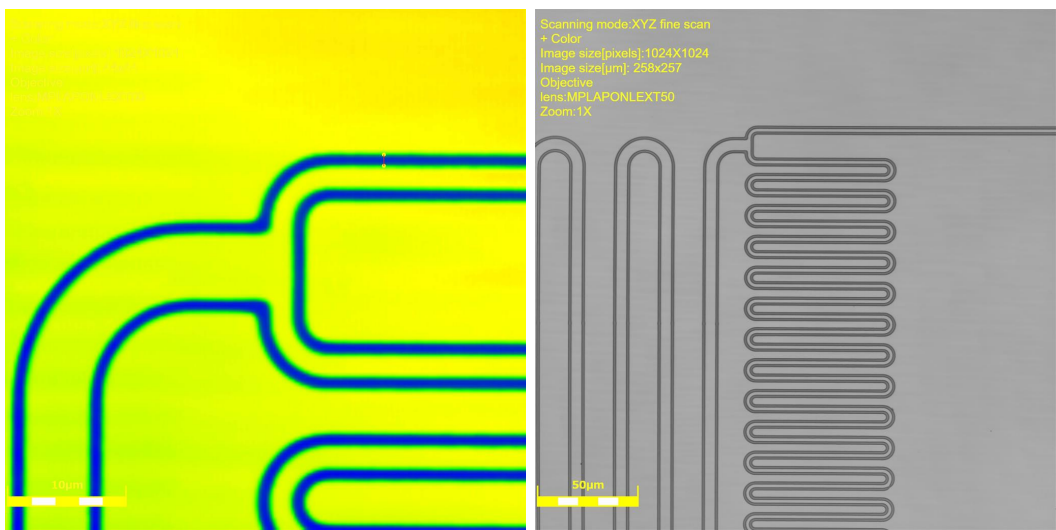


Figure 30: The design thickness is 1um, the real is 0.9um-1.1um.

The full dose test is presented in fig. 31.

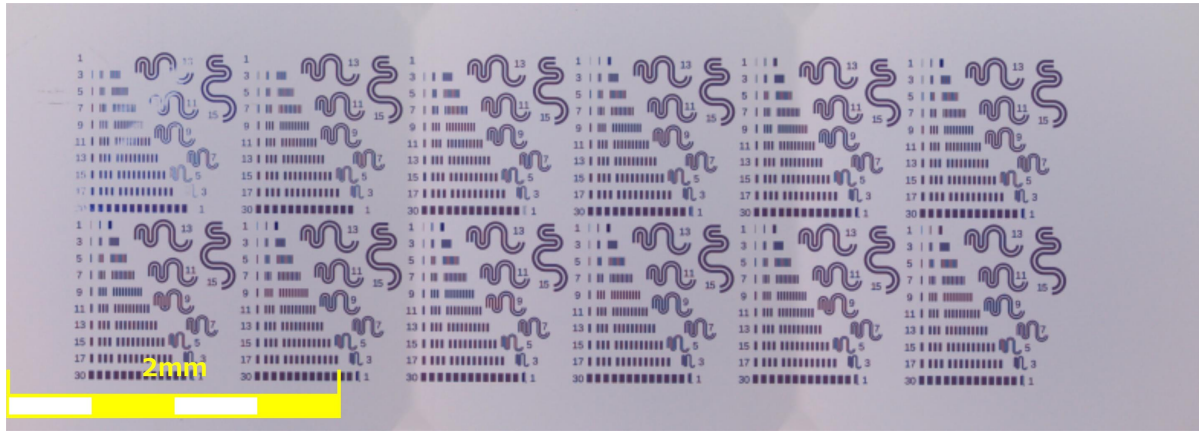


Figure 31: The full dose test of AZ resist. The dose range is  $47\text{-}105\text{mJ/cm}^2$ .

The result is following: see fig. 32. The resolution is 1  $\mu\text{m}$  for optic resist! The dose is  $57\text{mJ/cm}^2$ .

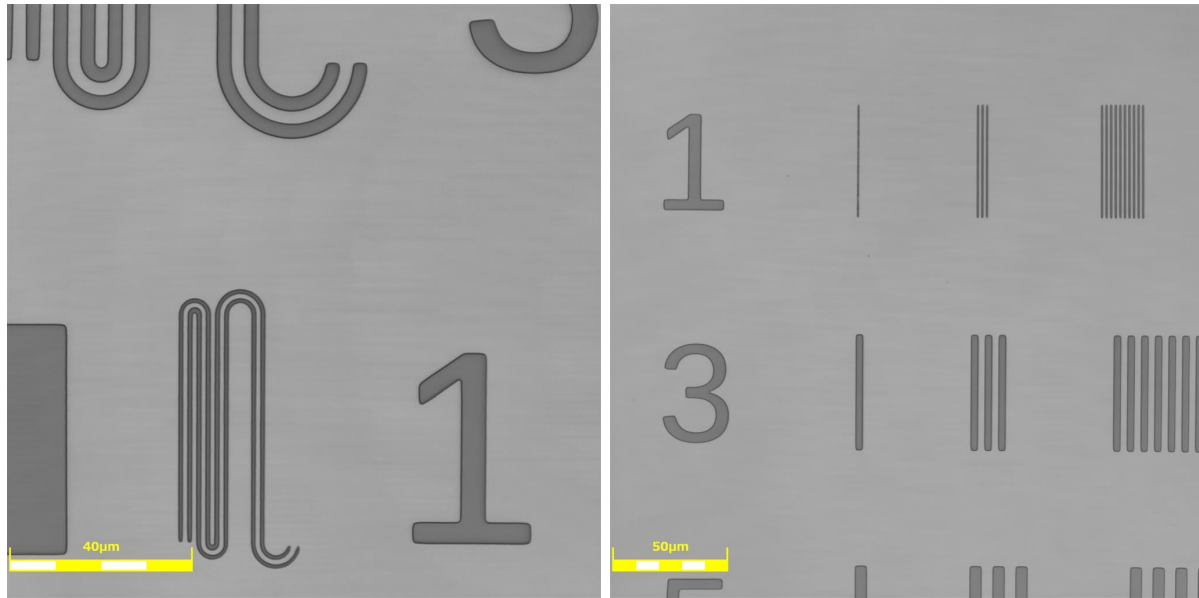


Figure 32: The best dose for dose test pattern.

The best dose for beam splitter pattern is  $70\text{mJ/cm}^2$ . As you can see the best dose is significantly different in comparison with different design pattern.

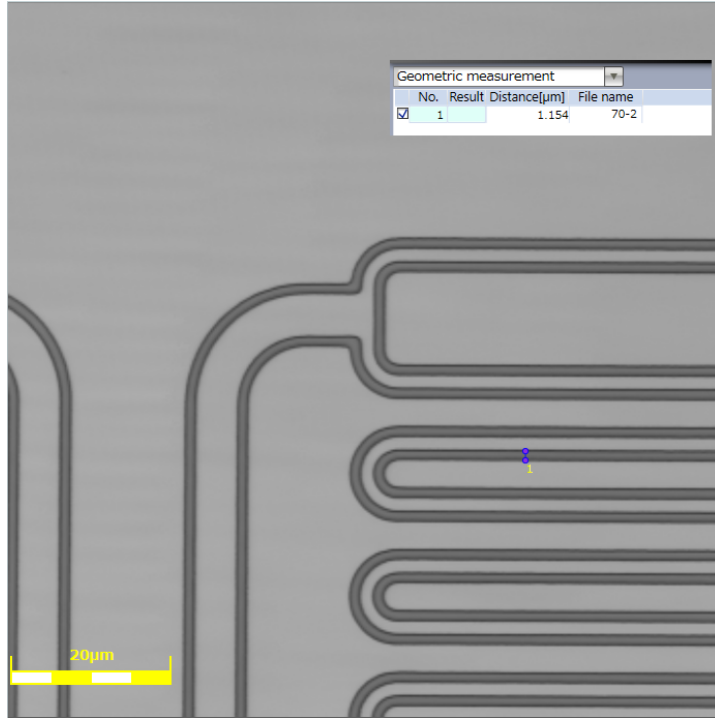


Figure 33: The best dose for beam splitter pattern. The width is 1.154um, the design width is 1 um. the exposure dose is  $70mJ/cm^2$ .

### 3.1 Airbridges fabrication

The fabrication process (the receipt you can find in my GitHub repository [2]) finishing by lift off. Actually, this receipt is just adapted version of the airbridge fabrication article [4]. There are some troubles with air bridges possible. The most complicated is cross-links (see fig. 34). Cross-links can appear only after finish resist remove, so we haven't information before liftoff. The beamsplitter#1 after aluminum etching and before dicing and resist remover is shown on fig. 35.

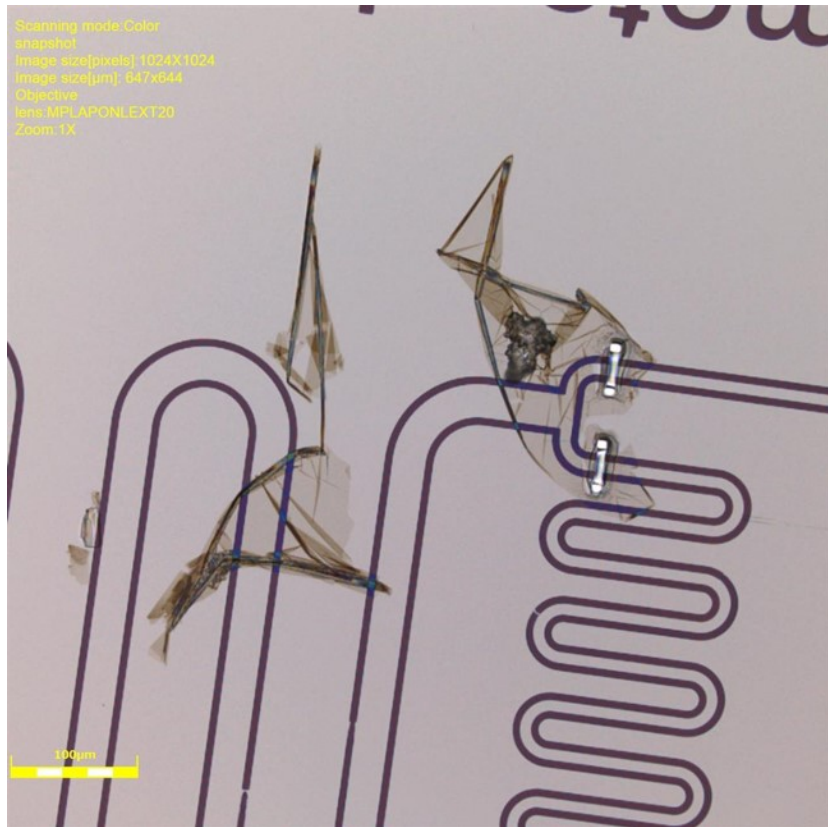


Figure 34: Cross-links problem after liftoff process. There are some polymerised organic film, that unetchable in oxygen plasma or liquid remover after its drying. This film hold on base of air bridges.

Reasons for cross-links occurring (i.e. polymerising):

1. Hot temperature 150 degree (not 140) during liftoff
2. Hot temperature during oxygen plasma
3. Using only single bath to liftoff (two is better).
4. Bad (no enough) plasma etching before aluminum etching (due to cross-links is typically for place near airbridge is based.)

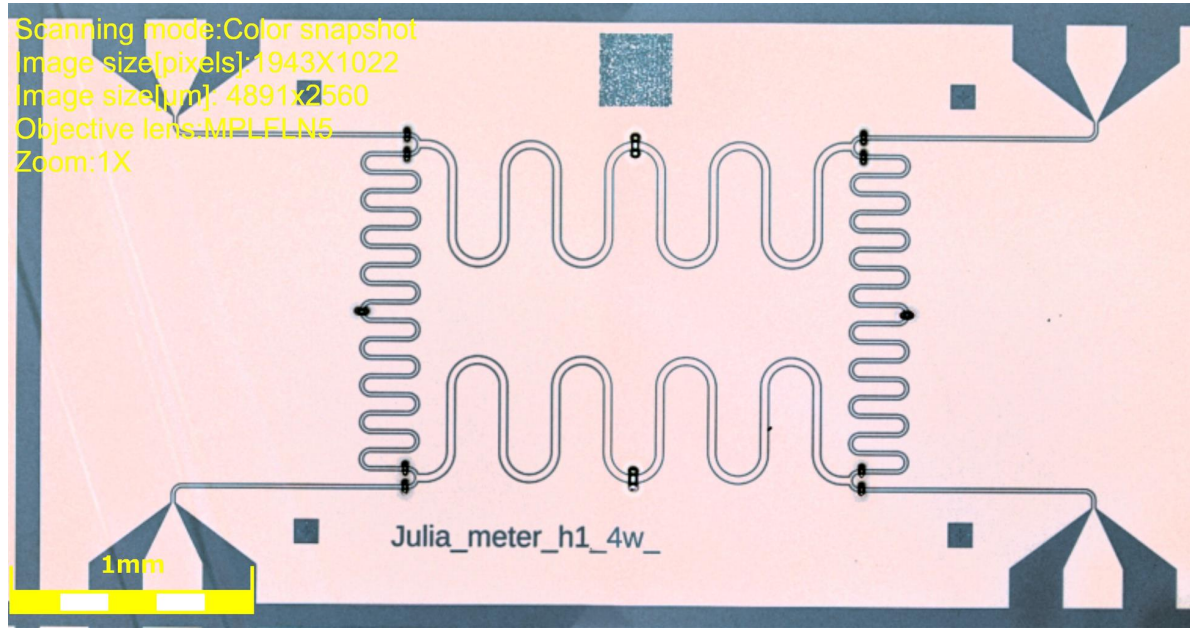


Figure 35: One of beam splitters #1 after aluminum etching (and oxygen ashing) and before dicing and liftoff.

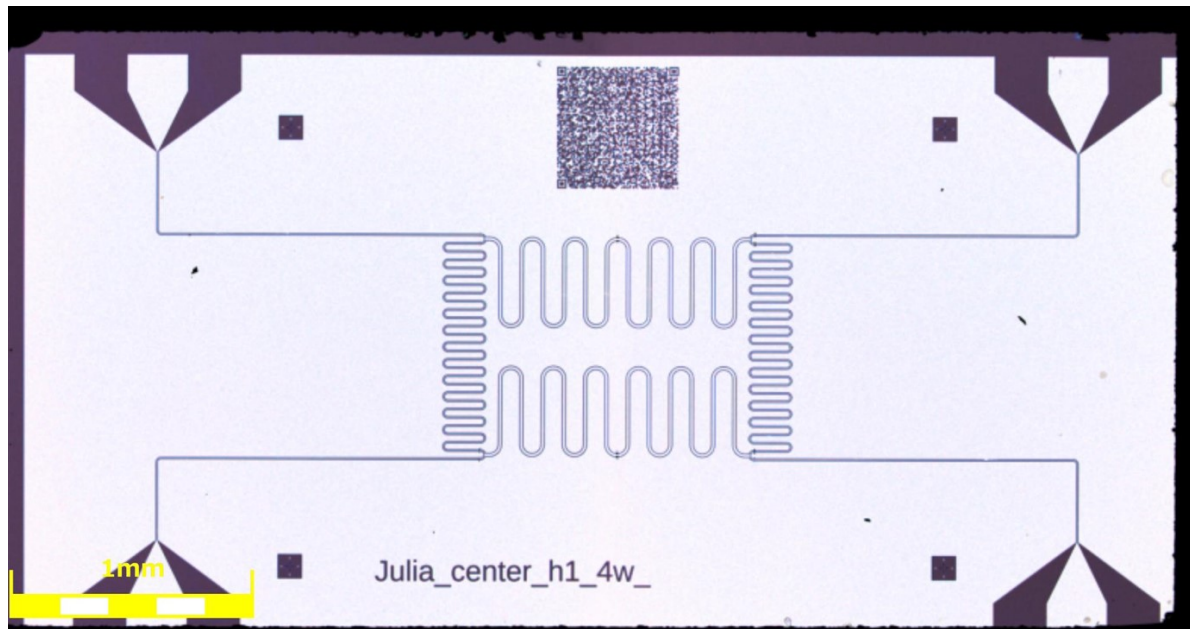


Figure 36: One of beam splitters #1 after liftoff.

Also, sometimes it is possible to remove cross-links using weak sonication bath (or sonication bath with placed one inside another to decrease output power). Due to approximately huge power airbridge just fly away. Some of airbridges from beam splitter #1 is shown in fig. 37. Typical sizes of airbridges are: length is (10um;50um), width is

(2um;10um), the thickness is 300nm (aluminum), the height is 3um.

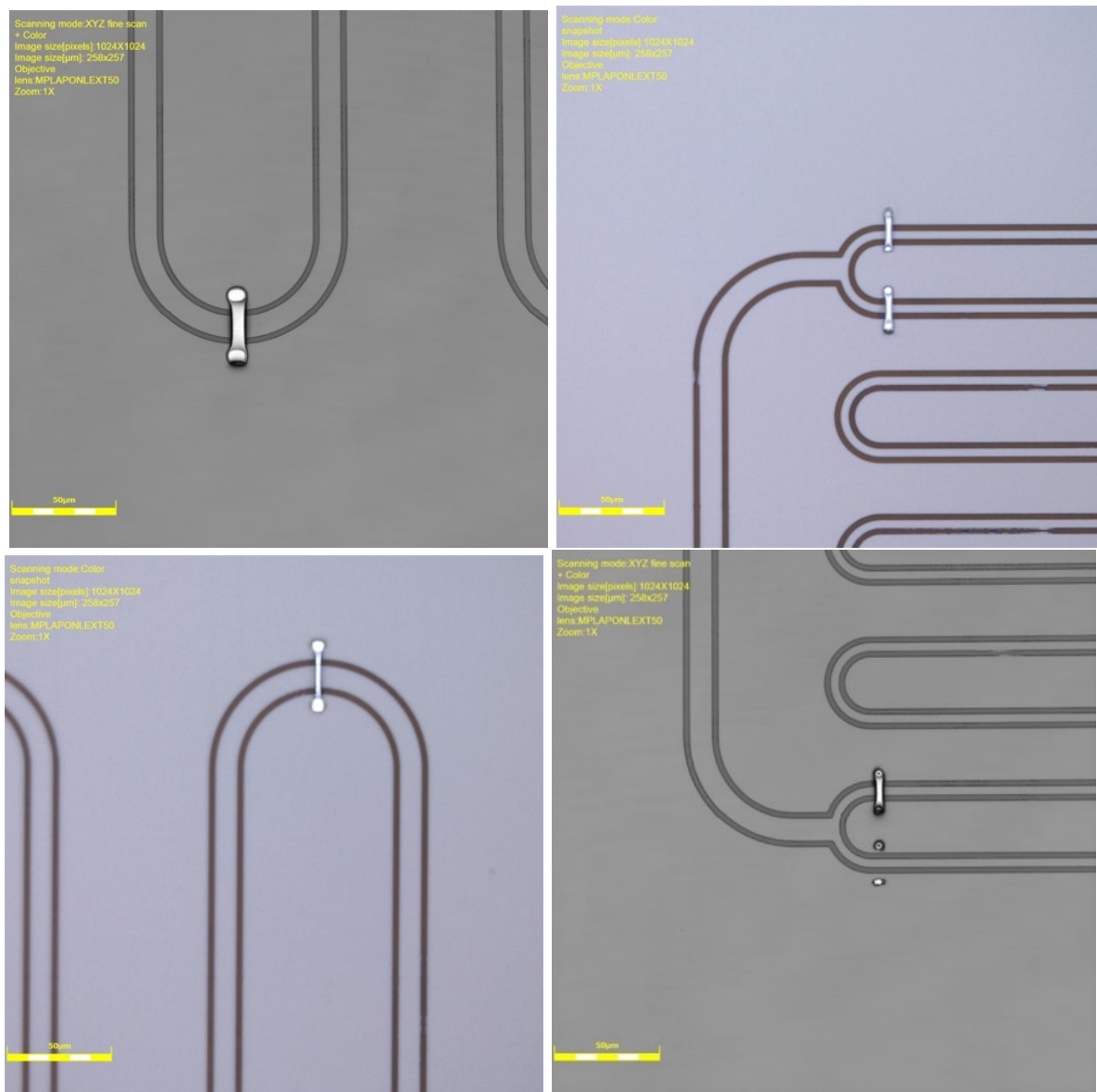


Figure 37: One of beam splitters #1 after liftoff.

#### Technical details:

1. In RIKEN optic maskless lithography system DL1000SG/RWS has permanent alignment shift of 1-2um.
2. After reflow process (to make specific arc shape of the resist) the size of airbridge changes – decrease on 1 um in any direction. For this case during airbridge design draw 1st layer – base of an airbridge should be bigger than 2nd layer.
3. Wet etching aluminum process will be longer and more unstable without fixing of

solvent temperature.

4. In RIKEN oxygen plasma machine Yamato has unstable plasma. For more reproducible process it should be make portion etching (like 5 times x 30 sec instead of 2 min). It can avoid huge heating too.
5. Lift off  $\frac{\text{should}+\text{must}}{2}$  do in solvent not hotter than 80C - to avoid abridge corruption (see fig. 38).
6. Weak sonication can help to avoid cross-links before them will be dried.

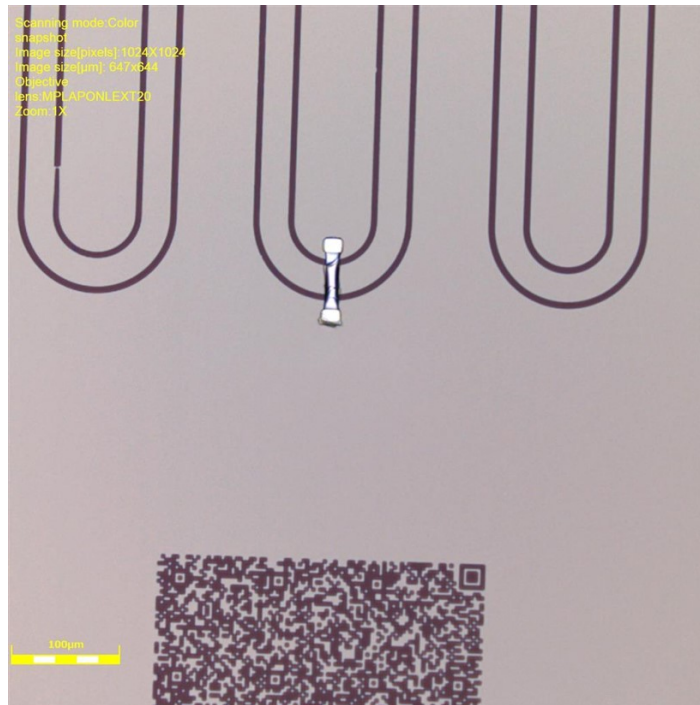


Figure 38: A corruption of an airbridge due to too hot remover.

### 3.2 Beam splitter#2

The new beamsplitter is used good wafer (100-1kOhms) from AIST and Peng. The design is changed due to it is required to increase sizes of airbridges. The difference is coplanar sizes of the gap 1um, 2.5um, 3.75um (instead of 0.55 um) and 5 um. Also, the absolute size of airbridge changed: total length = 1.3\*width feed line + 2\*pad length-3um.

Another difference is that oxygen plasma made by portion of 30 sec, in comparison with the first generation of beam splitter. In RIKEN aluminum etching solvent was finished and I have to finish my samples at Moscow. There oxygen etching was repeat in good and stable plasma and samples were finished. After liftoff there was no any problems like

cross-links as shown in fig. 41.

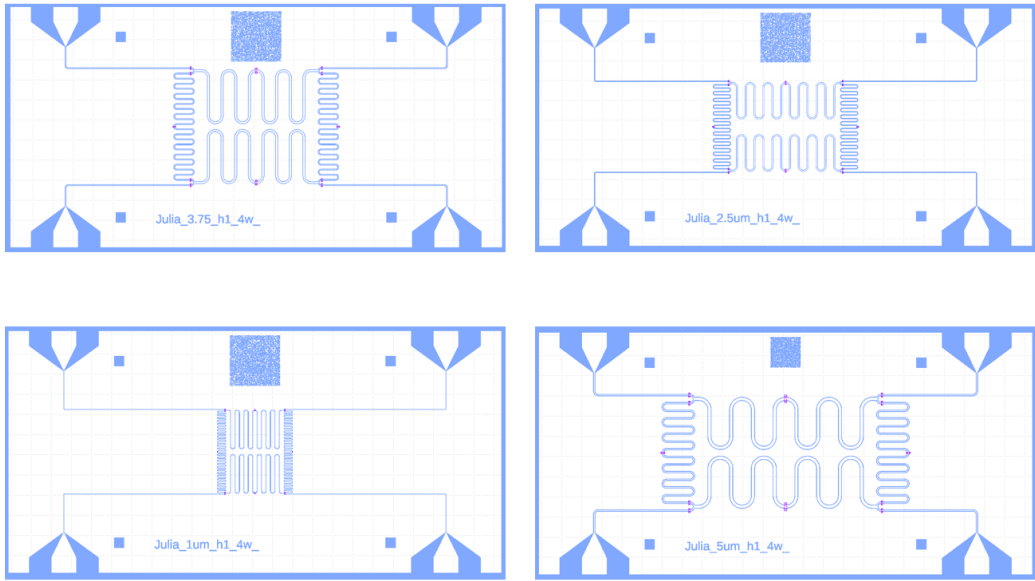


Figure 39: A new design of the second generation of beam splitters.

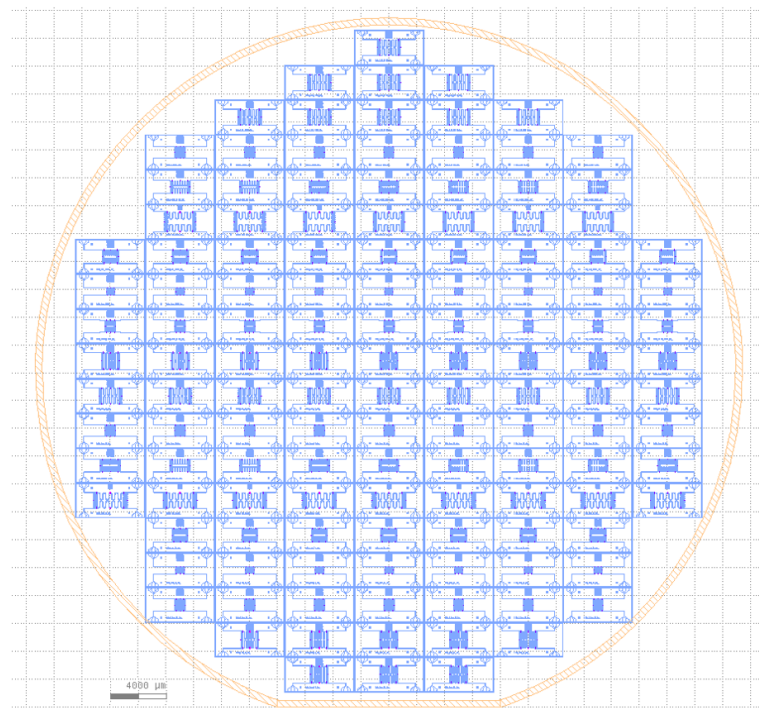


Figure 40: the Total new design of the second beamsplitter on 2-inch wafer.

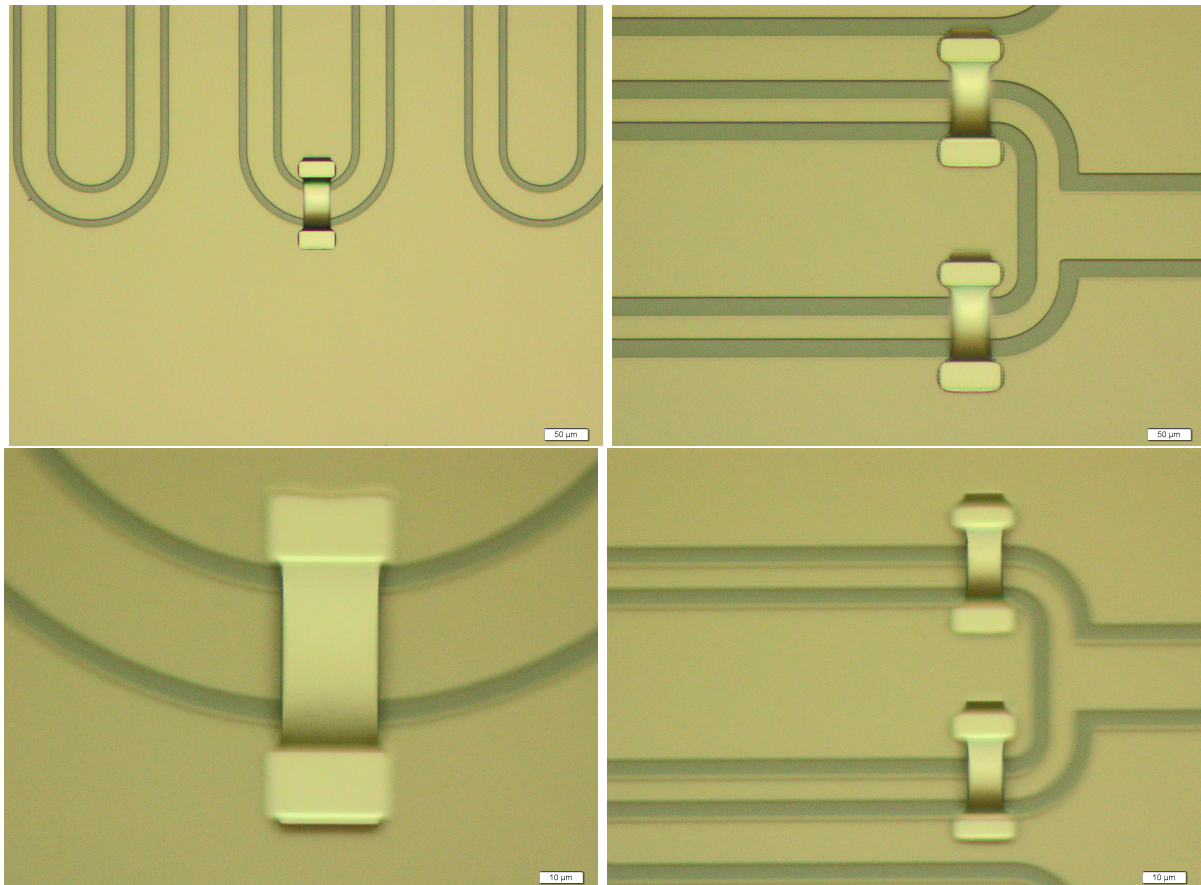


Figure 41: Example of the second generation of beam splitters after liftoff.

Consequently, it can be possible to say that poor etching plasma on the step exactly before aluminum etching one of the main reason of weak liftoff.

## 4 Measurement of a beamsplitter

The bonded sample is depicted in fig. 42. The sample's size is 5mm x 2.5mm. PCB from RIKEN that covered gold was used. From Russia the sample holder and others equipment that were used. The chip height of the chip is less than height of PCB hole – 450um vs 500um – so bonding takes more time than usual process.

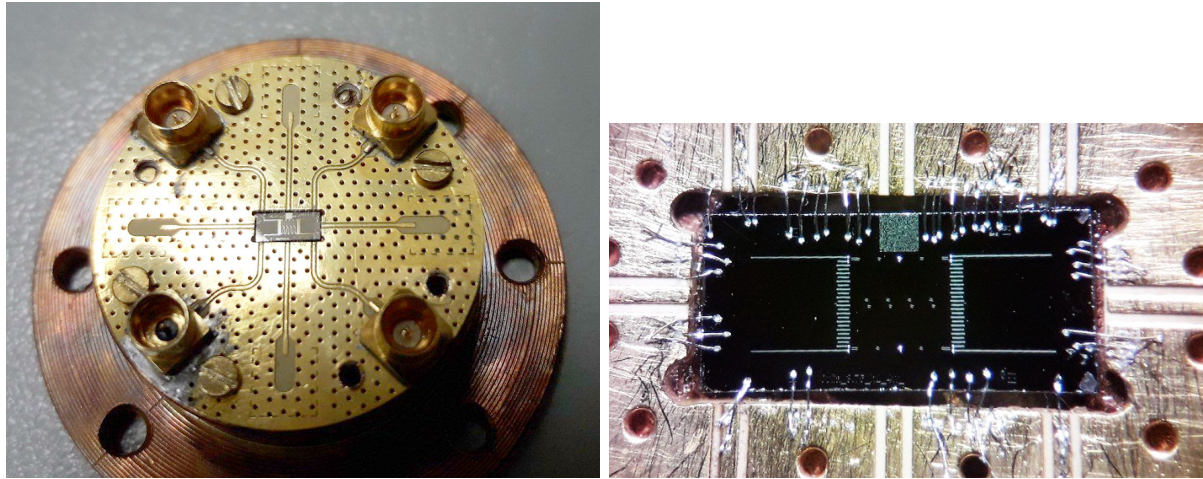


Figure 42: Optic photo of the bonded sample.

For the measurement scheme was used 3 cryo amplifiers, one circulator and 3 isolators. The measurement scheme is shown in fig. 43. Isolators are needed to prevent leakage of signal=heat, his work is similar with diod. The circulator is needed to prevent heat leakage too and to have an opportunity to measure reflection signal S11. The input line has number 1, output lines have numbers 1 and 2 – for transmission coefficient; 4 and 11 ( 11 without cryo amplifier) – for reflection. The amplification of the cryo amplifiers on 6 GHz are: output 1 [10K] 40dB, output 2 – [5K] – 40 dB, output 3 – [5K] – 40dB.

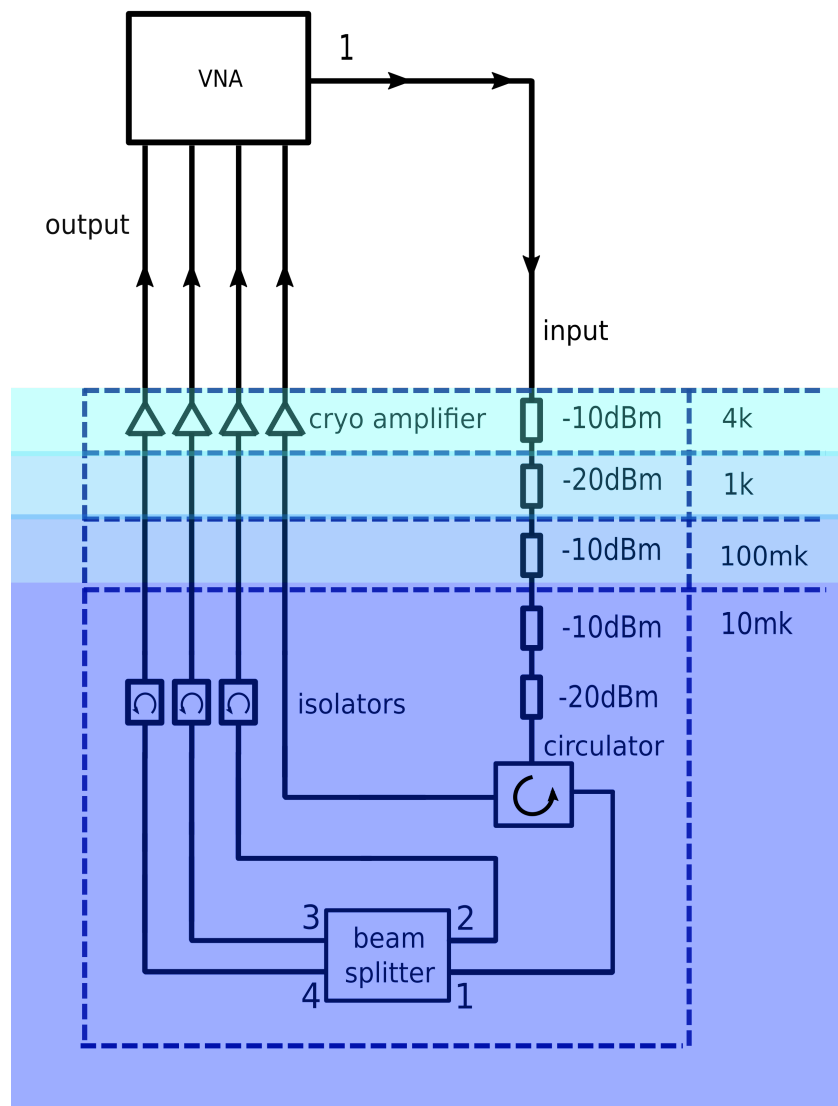


Figure 43: The measurement scheme of a beamsplitter

## 4.1 Measurement result

The raw measured results is here (see fig. 44).

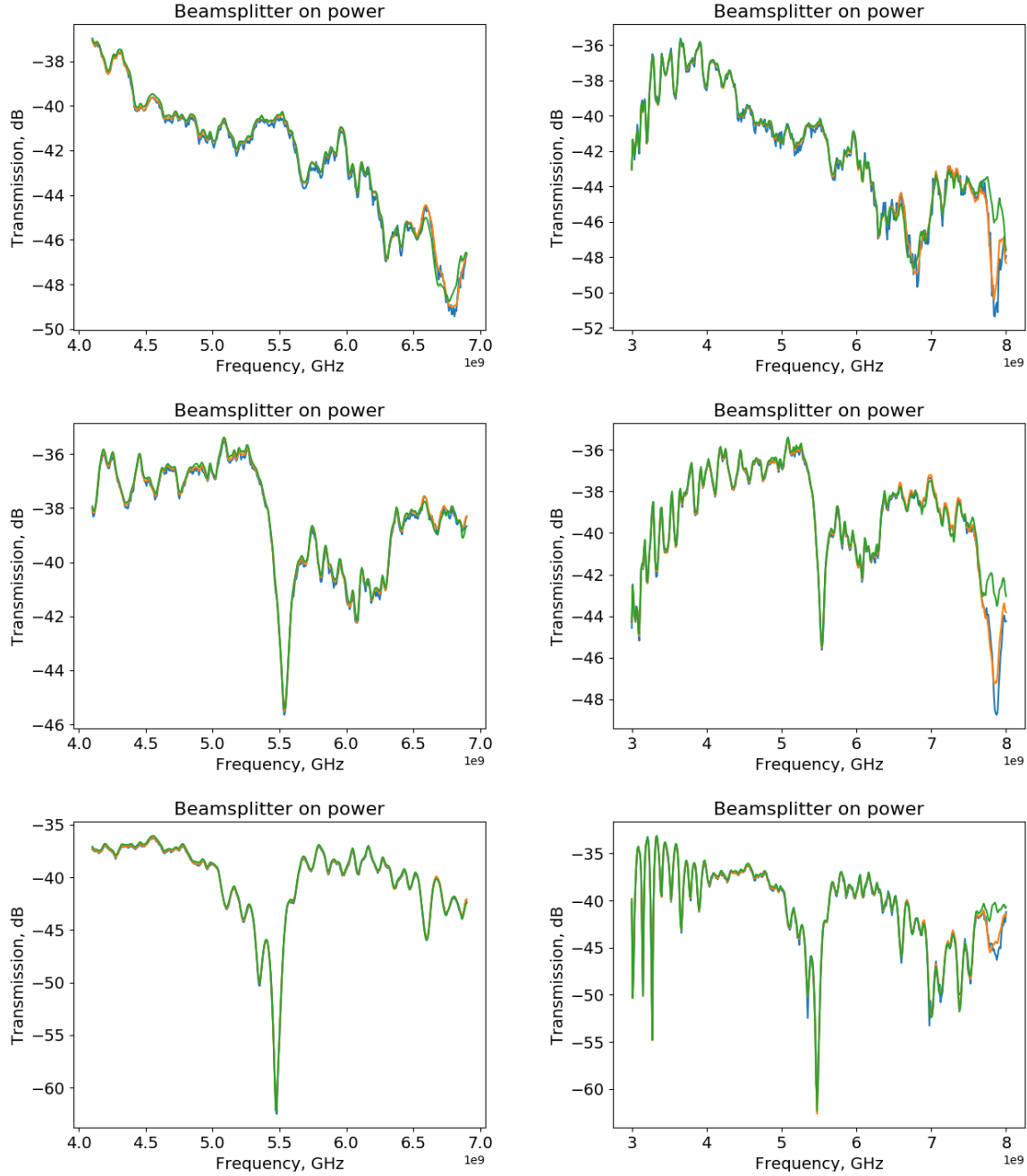


Figure 44: Measured characteristics of the beamsplitter: the top line is transmission signal, the central and the bottom line is reflection. The another transmission line is not measured due to technical problems (the pump has breaking down).

From reflection we can find that the central peak is in 5.5GHz instead of exactly 6GHz.

The quality of transmission will be understandable (for me personally) only after deduction of noises and grading from frequency dependence declining. The data processing is developing...waiting...

## References

- [1] Pozar David M. Microwave engineering. — John Wiley & Sons, 2009.
- [2] Zotova Julia. GitHub folder for macros design and the latest version of this text. — Access mode: <https://github.com/juzotova/BosonSampling>.
- [3] Rosu Iulian. Microstrip, stripline, and CPW Design // YO3DAC / VA3IUL, <http://www.qsl.net/va3iul>.
- [4] Fabrication and characterization of aluminum airbridges for superconducting microwave circuits / Zijun Chen, Anthony Megrant, Julian Kelly et al. // Applied Physics Letters. — 2014. — Vol. 104, no. 5. — P. 052602.